Cellulose (2014) 21:879–884
DOI 10.1007/s10570-013-0051-z

ORIGINAL PAPER

Effect of microfibril twisting on theoretical powder diffraction patterns of cellulose Iβ

Jodi A. Hadden · Alfred D. French · Robert J. Woods

Received: 17 May 2013 / Accepted: 11 September 2013 / Published online: 25 September 2013

Abstract Previous studies of calculated diffraction patterns for cellulose crystallites suggest that distortions that arise once models have been subjected to molecular dynamics (MD) simulation are the result of both microfibril twisting and changes in unit cell dimensions induced by the empirical force field; to date, it has not been possible to separate the individual contributions of these effects. To provide a better understanding of how twisting manifests in diffraction data, the present study demonstrates a method for generating twisted and linear cellulose structures that can be compared without the bias of dimensional changes, allowing assessment of the impact of twisting alone. Analysis of unit cell dimensions, microfibril volume, hydrogen bond patterns, glycosidic torsion angles, and hydroxymethyl group orientations confirmed that the twisted and linear structures collected with this method were internally consistent, and theoretical powder diffraction patterns for the two were shown to be effectively indistinguishable. These results indicate that differences between calculated patterns for the crystal coordinates and twisted structures from MD simulation can result entirely from changes in unit cell dimensions, and not from microfibril twisting. Although powder diffraction patterns for models in the 81-chain size regime were shown to be unaffected by twisting, suggesting that a modest degree of twist is not inconsistent with available crystallographic data, it may be that other diffraction techniques are capable of detecting this structural difference. Until such time as definitive experimental evidence comes to light, the results of this study suggest that both twisted and linear microfibrils may represent an appropriate model for cellulose Iβ.

Keywords Cellulose · Microfibril twist · Molecular dynamics · X-ray diffraction

J. A. Hadden · R. J. Woods (✉)
Complex Carbohydrate Center, University of Georgia, 315 Riverbend Road, Athens, GA 30602, USA
e-mail: rwoods@ccrc.uga.edu

A. D. French
Southern Regional Research Center, U.S. Department of Agriculture, 1100 Robert E. Lee Boulevard, New Orleans, LA 70124, USA

R. J. Woods
School of Chemistry, National University of Ireland, Galway, University Road, Galway, Ireland

Introduction

Just over a decade ago, Nishiyama et al. (2002) combined X-ray and neutron diffraction data to develop a high-resolution crystallographic structure of cellulose Iβ, describing it in terms of both heavy and hydrogen atom positions. This structure, based on samples of tunicin, is characterized by an ordered array of perfectly parallel glucosyl chains associated into layers by a well-defined hydrogen bond network (Fig. 1a). In recent years, molecular dynamics (MD) simulation studies of

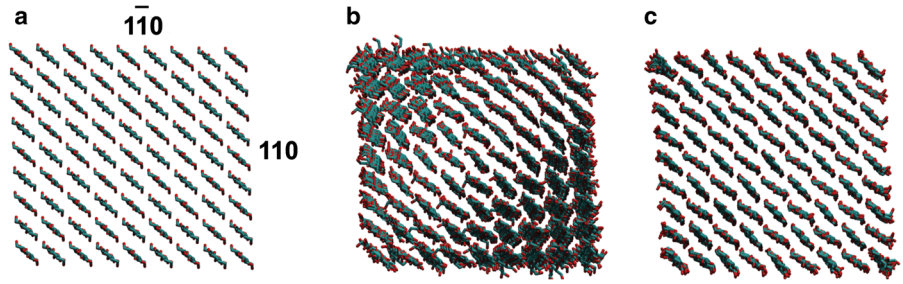

Fig. 1 View down the microfibril axis for **a** the crystallographic structure of cellulose Iβ, **b** a finite (twisted) structure, and **c** an infinite (linearly constrained) structure with chain termini bonded across the simulation box periodic boundary

finite or "mini-crystal" microfibril models based on these coordinates have demonstrated a preference to distort from the linearly oriented crystal structure and adopt a twisted conformation (Fig. 1b) (Bu et al. 2009; Glass et al. 2012; Hadden et al. 2013; Matthews et al. 2012; Matthews et al. 2011; Matthews et al. 2006; Paavilainen et al. 2011; Yui et al. 2006). While some experimental data supports the existence of twisted microfibrils (Hanley et al. 1997; Hirai et al. 1998), the apparent contradiction with high-resolution crystallographic data has been the source of considerable controversy in the cellulose structure community.

More recently, Nishiyama et al. (2012) published work comparing theoretical diffraction patterns for the crystallographic coordinates with those calculated from twisted structures produced by MD simulation. They observed significant changes in peak positions and intensities and attributed these distortions both to microfibril twisting and to changes in unit cell dimensions induced by the empirical force field. To separate the individual contributions of these two effects and provide a better understanding of how twisting in crystalline cellulose manifests in diffraction data, the present study demonstrates a method for generating twisted and linear cellulose structures that can be compared without the bias of dimensional changes. While the twisted structure represents a typical finitely modeled microfibril (Fig. 1b), the linear structure is constrained from twisting by bonding chain termini across the simulation box periodic boundary, making it essentially infinite (Fig. 1c). As the infinite model is nevertheless permitted to adapt to dimensional changes induced by the force field, it represents a linearly oriented form of cellulose Iβ, similar to the crystallographic structure, with unit cell dimensions that are comparable to those of the twisted form. Comparison of powder diffraction patterns calculated for these two structures thus allows an unbiased assessment of the impact of twisting alone.

Computational methods

Microfibril starting structures for MD simulations were prepared with Mercury 2.0 (Macrae et al. 2008), based on the cellulose Iβ crystallographic coordinates reported by Nishiyama et al. (2002). Models consisted of 81 total chains (9 per face), and were constructed such that the $1\bar{1}0$ and 110 planes formed the exposed surfaces (Fig. 1a). Finite microfibrils were generated with 20 glucosyl units per chain [degree of polymerization (DP) 20], while infinite microfibrils were generated with DP 18, with terminal residues bonded across the simulation box periodic boundary. Models were surrounded with a 12 Å solvent buffer.

Microfibrils were parameterized with the GLYCAM06 (Kirschner et al. 2008) (version h) force field for carbohydrates, and solvent was modeled as TIP3P water (Jorgensen et al. 1983). Simulation files were generated using the tleap module of AmberTools12 (Case et al. 2012), and subsequently converted to GROMACS format with the glycam2gmx.pl script from Wehle et al. (2012). The double precision parallel implementation of the mdrun module from GROMACS 4.5.5 (Berendsen et al. 1995; Hess et al. 2008; van der Spoel et al. 2005) was employed for all simulation work.

An energy minimization protocol consisting of 12,500 cycles of steepest descent, followed by 12,500 cycles of conjugate gradient, was applied to the solvent and subsequently to the entire system prior to the start of dynamics. MD simulations were performed under isothermal, isobaric (NPT) conditions utilizing Berendsen thermo- and barostats (time constants of 1 ps) to maintain a reference temperature of 300 K and pressure of 1 bar. A nonbonded cutoff of 8 Å was applied, beyond which van der Waals interactions were truncated and long-range electrostatics were handled with particle mesh Ewald (Darden et al. 1993). Covalent bonds to hydrogen were constrained using the LINCS algorithm (Hess et al. 1997) to allow

a simulation time step of 2 fs. Systems were equilibrated for 1 ns, followed by 10 ns of production dynamics. The periodic-molecules option was set for the infinite microfibril model to allow coupling of chain termini across the periodic boundary.

GROMACS trajectories were converted to AMBER format for analysis using VMD (Humphrey et al. 1996). Water molecules were removed, and microfibril models were cropped to contain only the center 16 glucose repeats (DP 16). This ensured comparison between models of equivalent dimension, as well eliminated noise resulting from terminal fraying during simulation of the finite model. Unit cell dimensions, hydrogen bond percentages, glycosidic torsion angles, and hydroxymethyl group orientations were determined using the ptraj module of AmberTools12 (Case et al. 2012). Average microfibril volume was calculated with Mol_Volume (Balaeff 2013), based on 100 evenly spaced frames extracted from simulation trajectories. Theoretical powder diffraction patterns were calculated with Debyer (Wojdyr 2012) for this ensemble of 100 trajectory frames, employing a value of $\lambda = 1.5418$ Å to denote CuKα radiation. Reference patterns for the crystallographic coordinates were calculated with Mercury 2.0 (Macrae et al. 2008), which assumes an infinite crystallite size and eliminates artifacts associated with low angle scattering seen in patterns calculated with Debyer.

Twisting was quantified using the metric for calculating θ_{Twist} defined by Hadden et al. (2013). This method designates two vectors (v, u) across the microfibril $1\bar{1}0$ face, perpendicular to the axis. While the vectors are parallel in the linear starting structure, their dot product describes the angle by which they diverge as the microfibril twists (Eq. 1).

$$\theta_{Twist} = \frac{180}{\pi} cos^{-1} \frac{v \cdot u}{|v||u|} \quad (1)$$

Values of θ_{Twist} were normalized by the number of cellobiose repeats between the vectors and averaged over time to give $\langle \theta_{Twist} \rangle$.

Results and discussion

MD simulations were performed on the 10 ns timescale for finite (twisted, Fig. 1b) and infinite (linearly constrained, Fig. 1c) cellulose microfibrils. The twisted structure displayed a $\langle \theta_{Twist} \rangle$ value of 1.17° per cellobiose, with root-mean-squared fluctuation of 0.14° and standard deviation of the mean of 0.02°. Although the unit cell showed some deviation from the crystallographic coordinates in all three dimensions (−1.3 % in **a**, +0.5 % in **b**, and +4.0 % in **c**), as has previously been observed during simulations of cellulose microfibrils (Matthews et al. 2006), there were no significant differences in dimensions between the twisted and linear structures. Values for microfibril volume showed an increase of approximately 5 % from the crystallographic coordinates, yet corresponded exactly for the two MD models. Additionally, the twisted and linear structures contained equivalent, as well as experimentally consistent, internal hydrogen bond patterns, glycosidic torsion angles, and hydroxymethyl group orientations. These data are summarized in Tables 1 and 2, and together indicate that with the exception of twisting, the twisted and linear structures produced with this method are essentially identical, allowing for straightforward, unbiased comparison of theoretical diffraction data.

Powder diffraction patterns calculated based on the final frames of simulation trajectories for both the twisted and linear microfibrils are presented in Fig. 2, along with three reference patterns corresponding to the original crystallographic coordinates. The lower two reference patterns assume infinite crystallite size,

Table 1 Values used for quantitative comparison of twisted and linear microfibril models

Model	$\langle \theta_{Twist} \rangle$ (°)	Unit cell dimensions (Å)						Volume ($\times 10^5$, Å^3)	200 2-θ (°)	PWHM (°)
		a	RMSF[a]	b	RMSF	c	RMSF			
Twisted	1.17	7.69	0.18	8.24	0.15	10.80	0.10	1.97	23.24	1.75
Linear	–	7.68	0.17	8.24	0.14	10.79	0.09	1.97	23.27	1.75
Iβ crystal	–	7.78	–	8.20	–	10.38	–	1.87	22.98	1.64

[a] Root-mean-squared fluctuation

Table 2 Values used for quantitative comparison of twisted and linear microfibril models

Model	Hydrogen bonds (%)			ϕ (°)	RMSF[a]	ψ (°)	RMSF	Hydroxymethyl group (%)		
	H_2O–O_6	H_3O–O_5	H_6O–O_3					tg	gt	gg
Twisted	99.6	99.7	98.5	27.2	6.7	−24.3	6.8	98.4	1.3	0.3
Linear	99.4	99.5	98.4	26.8	6.7	−24.3	6.8	99.3	0.6	0.1
Iβ crystal	100	100	100	23.9	–	−27.4	–	100	0	0

[a] Root-mean-squared fluctuation

and demonstrate the absence of artifacts associated with low angle scattering present in the remaining patterns, which were calculated based on non-periodic 81-chain, DP 16 mini-crystals. This is especially obvious in the 10°–13° region of 2-θ. The upper reference pattern was calculated in an identical manner to that of the twisted and linear models and provides a direct comparison to assess distortions arising from MD simulation.

While the patterns for the twisted and linear structures indeed display distortions relative to that of the crystallographic structure, as previously discussed by Nishiyama et al. (2012), they are effectively indistinguishable from each other. The PWHM for the 200 peak (averaged over patterns for 100 simulation frames) was equivalent for the two MD models, but

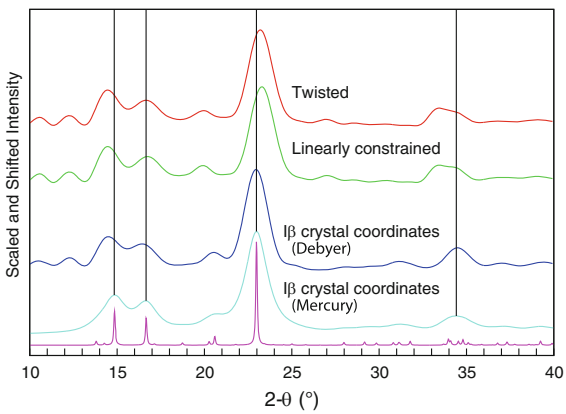

Fig. 2 Theoretical powder diffraction patterns for twisted and linear microfibril models and three reference patterns corresponding to the original crystallographic coordinates for cellulose Iβ. The *upper* three patterns were calculated with Debyer (Wojdyr 2012) as non-periodic 81-chain, DP 16 mini-crystals, while the *lower* two patterns were calculated with Mercury 2.0 (Macrae et al. 2008) with the assumption of infinite crystallite size (PWHM of 0.1° and 1.5°) to demonstrate the absence of artifacts associated with low angle scattering present in the Debyer patterns. Peak heights were each normalized to 100

was broader (by less than 10 %) than that of the crystal coordinates, with the value for 2-θ shifted by less than 2 % (Table 1). Because the twisted and linear structures give rise to equivalent theoretical diffraction patterns, the distortions relative to the pattern for the crystallographic structure must arise from dimensional changes induced by the force field during simulation, as suggested by Nishiyama et al. (2012), and not from microfibril twisting. This is expected to hold for all microfibrils, provided that the model is large enough that twisting does not excessively disorder the unit cell of the crystalline assembly.

As discussed by Nishiyama et al. (2012), low-angle scattering can influence both peak position and intensity, in particular for the $1\bar{1}0$ reflection at 14.5° 2-θ. While some low-angle scattering can manifest in experimental patterns as a result of discontinuity between crystallites or inhomogeneity in the sample, the extent of it observed in the present theoretical patterns represents the worst-case scenario for non-periodic models of this size. Along with issues of preferred orientation of crystals in experimental patterns, low-angle scattering may present a greater concern for making comparisons between theory and experiment than modest twisting.

While this study has demonstrated that powder patterns are unaffected by a limited degree of microfibril twisting, it may be that other experimental techniques are capable of detecting this subtle structural difference. For example, Nishiyama et al. (2012) presented theoretical fiber diffraction patterns that displayed wedge-shaped layer lines for twisted models that were not subjected to convolution to account for crystallite tilt distribution. These wedges were shown to have larger angles for models with fewer numbers of chains, which display a greater degree of twisting. It should be noted, however, that the models used in that study were relatively small compared to the tunicate samples (10–20 nm) used to solve the cellulose Iβ

crystal structure. Hadden et al. (2013) estimated that twisted microfibrils observed experimentally by Hanley et al. (1997), which ranged in size from 20 to 50 nm, likely would have had a uniform twist of only 0.26° per cellobiose when suspended in aqueous solution. This observation suggests that the degree of twisting present in large samples, such as those used for X-ray diffraction, is sufficiently subtle that it may be difficult to detect experimentally. Even with the use of comparatively small microfibril models, both the present work and that of Nishiyama et al. (2012) imply that a modest degree of twisting is not necessarily inconsistent with crystallographic data.

Conclusions

The method presented here for generating internally consistent twisted and linear structures provides a previously unexploited strategy for probing the effect of microfibril twisting on experimental cellulose diffraction data. While this study has demonstrated that theoretical powder patterns for models in the 81-chain size regime are unaffected by twisting, suggesting that a modest degree of twist is not inconsistent with available crystallographic data, it may be that other diffraction techniques are capable of detecting this subtle structural difference. Further analysis is thus required to assess the effect of twisting on other back-calculated diffraction properties, as well as to confirm these observations experimentally. Until such time as definitive experimental evidence comes to light, the results of this study suggest that both twisted and linear microfibrils may represent an appropriate model for cellulose Iβ.

Acknowledgments The authors are grateful to Cotton, Inc. for support of this work, as well as the National Institutes for Health (GM094919 (EUREKA)) and the Science Foundation of Ireland (08/IN.1/B2070).

References

Balaeff A (2013) Mol_Volume. http://wwwksuiucedu/Development/MDTools/molvolume/

Berendsen HJC, Vanderspoel D, Vandrunen R (1995) Gromacs—a message-passing parallel molecular-dynamics implementation. Comput Phys Commun 91(1–3):43–56

Bu LT, Beckham GT, Crowley MF, Chang CH, Matthews JF, Bomble YJ, Adney WS, Himmel ME, Nimlos MR (2009) The energy landscape for the interaction of the family 1 carbohydrate-binding module and the cellulose surface is altered by hydrolyzed glycosidic bonds. J Phys Chem B 113(31):10994–11002

Case DA, Macke TJ, Svrcek-Seiler WA, Brown RA, Kolossváry I, Bomble YJ, Anandakrishnan R, Zhang W, Hou T, Schafmeister C, Ross WS, Wang J, Wolf RM, Cheatham TE III, Tsui V, Pitera JW, Gohlke H, Tanner S, Absgarten E, Roe DR, Frybarger P, Wang J, Cai Q, Ye X, Hsieh MJ, Tan C, Luo R, Walker RC, Crowley MF, Brozell S, Giese T, Götz AW, Lee TS, Williamson M, Luchko T, Gusarov S, Kovalenko A, Cerutti DS, Swails J, McGee TD Jr, Miller B III, Peters M, Ayers K, Wollacott A, Williams DE, Roberts BP, Merz KM Jr, Betz R (2012) AmberTools 12. University of California, San Francisco

Darden T, York D, Pedersen L (1993) Particle mesh Ewald: an N·log (N) method for Ewald sums in large systems. J Chem Phys 98:10089

Glass DC, Moritsugu K, Cheng XL, Smith JC (2012) REACH coarse-grained simulation of a cellulose fiber. Biomacromolecules 13(9):2634–2644

Hadden JA, French AD, Woods RJ (2013) Unraveling cellulose microfibrils: a twisted tale. Biopolymers 99(10):746–756

Hanley SJ, Revol JF, Godbout L, Gray DG (1997) Atomic force microscopy and transmission electron microscopy of cellulose from Micrasterias denticulata; evidence for a chiral helical microfibril twist. Cellulose 4(3):209–220

Hess B, Bekker H, Berendsen HJC, Fraaije J (1997) LINCS: a linear constraint solver for molecular simulations. J Comput Chem 18(12):1463–1472

Hess B, Kutzner C, van der Spoel D, Lindahl E (2008) GROMACS 4: algorithms for highly efficient, load-balanced, and scalable molecular simulation. J Chem Theory Comput 4(3):435–447

Hirai A, Tsuji M, Horii F (1998) Helical sense of ribbon assemblies and splayed microfibrils of bacterial cellulose. Senri Gakkai shi 54(10):506–510

Humphrey W, Dalke A, Schulten K (1996) VMD: visual molecular dynamics. J Mol Graph 14(1):33–38

Jorgensen WL, Chandrasekhar J, Madura JD, Impey RW, Klein ML (1983) Comparison of simple potential functions for simulating liquid water. J Chem Phys 79(2):926–935

Kirschner KN, Yongye AB, Tschampel SM, Gonzalez-Outeirino J, Daniels CR, Foley BL, Woods RJ (2008) GLYCAM06: a generalizable biomolecular force field. Carbohydrates. J Comput Chem 29(4):622–655

Macrae CF, Bruno IJ, Chisholm JA, Edgington PR, McCabe P, Pidcock E, Rodriguez-Monge L, Taylor R, van de Streek J, Wood PA (2008) Mercury CSD 2.0—new features for the visualization and investigation of crystal structures. J Appl Crystallogr 41:466–470

Matthews JF, Skopec CE, Mason PE, Zuccato P, Torget RW, Sugiyama J, Himmel ME, Brady JW (2006) Computer simulation studies of microcrystalline cellulose I beta. Carbohydr Res 341(1):138–152

Matthews JF, Bergenstrahle M, Beckham GT, Himmel ME, Nimlos MR, Brady JW, Crowley MF (2011) High-temperature behavior of cellulose I. J Phys Chem B 115(10):2155–2166

Matthews JF, Beckham GT, Bergenstrahle-Wohlert M, Brady JW, Himmel ME, Crowley MF (2012) Comparison of cellulose I beta simulations with three carbohydrate force fields. J Chem Theory Comput 8(2):735–748

Nishiyama Y, Langan P, Chanzy H (2002) Crystal structure and hydrogen-bonding system in cellulose 1 beta from synchrotron X-ray and neutron fiber diffraction. J Am Chem Soc 124(31):9074–9082

Nishiyama Y, Johnson GP, French AD (2012) Diffraction from nonperiodic models of cellulose crystals. Cellulose 19(2): 319–336

Paavilainen S, Rog T, Vattulainen I (2011) Analysis of twisting of cellulose nanofibrils in atomistic molecular dynamics simulations. J Phys Chem B 115(14):3747–3755

van der Spoel D, Lindahl E, Hess B, Groenhof G, Mark AE, Berendsen HJC (2005) GROMACS: fast, flexible and free. J Comp Chem 26:1701–1718

Wehle M, Vilotijevic I, Lipowsky R, Seeberger PH, Varon Silva D, Santer M (2012) Mechanical compressibility of the glycosylphosphatidylinositol(GPI) anchor backbone by independent glycosidic linkages. J Am Chem Soc 134(46): 18964–18972

Wojdyr M (2012) Debyer. http://wwwunipresswawpl/debyer, http://codegooglecom/p/debyer/wiki/debyer

Yui T, Nishimura S, Akiba S, Hayashi S (2006) Swelling behavior of the cellulose I beta crystal models by molecular dynamics. Carbohydr Res 341(15):2521–2530